Cement and Concrete Research 38 (2008) 745–750

Contents lists available at ScienceDirect

Cement and Concrete Research

journal homepage: http://ees.elsevier.com/CEMCON/default.asp

Surface carbonation of synthetic C-S-H samples: A comparison between fresh and aged C-S-H using X-ray photoelectron spectroscopy

Leon Black [a,b,*], Krassimir Garbev [c], Ian Gee [b,d]

[a] School of Civil Engineering, University of Leeds, Leeds, LS2 9JT, UK
[b] Materials and Engineering Research Institute, Sheffield Hallam University, Howard Street, Sheffield, S1 1WB, UK
[c] Forschungszentrum Karlsruhe GmbH, Institut für Technische Chemie, Bereich Thermische Abfallbehandlung (ITC-TAB), Hermann-von-Helmholtz-Platz 1, 76344 Eggenstein-Leopoldshafen, Germany
[d] Pera Group, Pera Innovation Park, Melton Mowbray, Leicestershire, LE13 0PB, UK

ARTICLE INFO

Article history:
Received 23 July 2007
Accepted 19 February 2008

Keywords:
Calcium-silicate-hydrate (C-S-H)
Carbonation
Crystal structure
X-ray photoelectron spectroscopy

ABSTRACT

This paper presents a continuation of studies into silicate anion structure using X-ray photoelectron spectroscopy (XPS). A series of C-S-H samples have been prepared mechanochemically, and then stored under ambient conditions for six months. Storage led to surface carbonation, the extent of which was dependent upon the calcium/silicon ratio of the fresh sample. Carbonation arose through decalcification of the C-S-H, leading to increased silicate polymerisation. The surfaces of the most calcium-rich phases (C/S = 1.33 and 1.50) underwent complete decalcification to yield silica (possibly containing some silanol groups) and calcium carbonate. Carbonation, and hence changes in silicate anion structure, was minimal for the C-S-H phases with C/S = 0.67 and 0.75.

1. Introduction

X-ray photoelectron spectroscopy (XPS) is a well-established technique for investigations of surface structure, and the technique has been thoroughly reviewed elsewhere [1]. It is possible, using XPS, to investigate the chemical state of all elements, excluding hydrogen, in a single experiment, giving a total analysis time per sample of about 1 to 2 h. Slight changes in the bonding environment of a given element results in changes in photoelectron spectra. For these reasons, XPS has proved itself suitable for structural examinations of C-S-H[1] gels.

Surface composition, as determined by XPS, has been shown to be applicable for the investigation of the bulk structure of calcium silicates [2–5] and calcium silicate hydrates [6–10]. Systematic changes in photoelectron spectra can be related to structural changes [11–13]. Increasing silicate anion polymerisation leads to increasing Si 2p binding energy [9–14], decreasing Ca 2p–Si 2p energy separation [2,6,2,4,6,9,10], decreasing modified Auger parameter [2,6,9,10,13] and a decreasing energy separation between the non-bridging and bridging oxygen atom components of the O 1s spectra [10,14].

We have recently used XPS to investigate fresh mechanochemically synthesised C-S-H samples with C/S ratios ranging from 0.4 to 1.5 [6]. The surface elemental composition was in good agreement with the bulk composition, and there were found to be systematic changes in photoelectron spectra with changes in C/S. The same samples have also been analysed using Raman spectroscopy, where systematic changes in the Raman spectra have been related to changes in silicate anion structure [15,16]. The fresh synthetic C-S-H phases were rapidly carbonated upon exposure to air, with the initial formation of amorphous calcium carbonate then aragonite and/or vaterite, together with silicate anion polymerisation [16]. The current work builds upon these earlier studies, using XPS to investigate the changes in silicate anion polymerisation upon ageing of mechanochemically prepared synthetic C-S-H phases. The surface sensitivity of XPS, with an information depth of about 5–10 nm, makes the technique ideally suited for investigations of surface phenomena. It is this capability which is exploited in this article, to look at C-S-H ageing under benign conditions.

There are various models proposed for the structure of C-S-H, many of which are based upon binary solid solutions. Taylor suggested that C-S-H gel consists of a mixture of nanometer sized 14 Å-tobermorite ($Ca_5[H_2Si_6O_{18}].8H_2O$) and jennite ($Ca_9[H_2Si_6O_{18}](OH)_8 \cdot 6H_2O$) domains [17,18]. Fujii and Kondo [19] initially considered C-S-H as a solid solution between tobermorite and portlandite. This was elaborated by Stade and Wieker [20] and Cong and Kirkpatrick [21], with the defect-tobermorite model, whereby variations in C/S ratio could be accommodated by defects in the tobermorite structure. The precise structure of C-S-H is system dependent [22], but a combination of the tobermorite–portlandite model and the tobermorite–jennite model adequately describes many systems, with the former being preferred in synthetic systems, and the latter in 'real' cement pastes.

Carbonation, the process by which cement reacts with atmospheric carbon dioxide, is primarily the reaction between portlandite and carbonic acid to form calcite. However, decalcification of the C-S-H can

* Corresponding author. School of Civil Engineering, University of Leeds, Leeds, LS2 9JT, UK. Tel.: +44 113 343 2283; fax: +44 113 343 2265.
E-mail address: l.black@leeds.ac.uk (L. Black).

[1] We have used standard cement chemistry nomenclature throughout this article, where C═CaO, S═SiO_2 and H═H_2O.

0008-8846/$ – see front matter © 2008 Elsevier Ltd. All rights reserved.
doi:10.1016/j.cemconres.2008.02.003

also occur [23–26], typically once the more ready source of calcium, portlandite, has been exhausted. C-S-H decalcification upon carbonation leads to silicate polymerisation, with the ultimate product being a silica gel and calcium carbonate [23,26]. The precise nature of the silica gel, however, is uncertain, although it is known to be highly polymerised, with a high Q^3 and Q^4 content [26].

The aim of this study has been to investigate the susceptibility to carbonation of various C-S-H phases of different C/S ratios. The highly surface sensitive technique of X-ray photoelectron spectroscopy has been used to examine the interface between the C-S-H paste and its environment, and thus determine the extent of surface carbonation, and hopefully the nature of the carbonation products.

2. Experimental

2.1. Synthesis

The nanocrystalline C-S-H phases were prepared mechanochemically, according to the method of Saito et al. [27] from stoichiometric mixtures of CaO (freshly prepared from $CaCO_3$ at 1000 °C for 5 h) and SiO_2 (Aerosil). Synthesis was performed using water/solid ratios of 8, with subsequent sample drying at 60 °C using a sub-boiling system. Further details have been provided elsewhere [10,15]. The following samples with target C/S-ratios were synthesised: C/S=0.4, 0.5, 0.67, 0.75, 0.83, 1.00, 1.33 and 1.50. Subsequent thermal analysis of the samples revealed a mass loss between 25 and 60 °C of between 6 and 10% for the samples, indicating some evidence of absorbed water in the samples [28].

After synthesis, and prior to analysis, the samples were stored under nitrogen in hermetically-closed glass vials. The first analysis was performed immediately after opening the vials and grinding the samples lightly with a pestle and mortar. A second set of samples were placed in plastic weighing boats and placed inside in a covered, not closed, desiccator for 6 months. This storage under ambient conditions allowed exposure to the atmosphere and air circulation, while preventing dust contamination.

2.2. Analysis

The powdered samples were taken from their sealed glass vials, a small amount of material pressed onto adhesive aluminium foil, mounted on a sample stub and introduced to the vacuum system of the spectrometer. The samples were analysed using an ESCA300 photoelectron spectrometer fitted with a high power rotating anode (8 kW) and monochromatised Al Kα (hν=1486.7 eV) X-ray source. The X-ray beam is focused onto a 6 mm×0.5 mm region on the sample via a large, seven crystal, double focusing monochromator. The Al Kα line profile has a FWHM energy width of 0.26 eV. The detection system consists of a 300 mm radius hemispherical analyser and a multi-channel detector. The system was operated with 0.8 mm slits and a 150 eV pass energy, giving an overall instrument resolution of 0.30 eV. The samples were often extremely good electrical insulators. It was therefore necessary to use a flood gun to compensate for sample charging.

3. Results and discussion

Fig. 1 shows the Si 2p, O 1s and C 1s spectra of the eight samples, fresh and after storage for six months. The Ca 2p spectra are not shown, as they showed no change upon ageing. This is not unexpected, as, with the exception of the phyllosilicates, many calcium-containing compounds have similar binding energies [6]. The aged samples did, however, show marked changes in their Si 2p spectra. These changes were slight for the phases with C/S≤0.75, with small shifts to higher binding energy, indicative of slight silicate polymerisation. The calcium-rich samples meanwhile exhibited much greater spectral changes upon ageing. All of the spectra exhibited a maximum at 103.2 eV, with there being some residual intensity at ~102 eV for the samples with C/S=0.83 and 1.00. This considerable shift indicates significant surface silicate anion polymerisation upon ageing, and a binding energy of 103.2 eV is characteristic of a highly polymerised silicate structure, e.g. silica [13]. This increased silicate polymerisation can also be seen when examining the O 1s spectra. The phases with C/S≤0.75 all show subtle changes upon ageing, with a slight loss in intensity at ~530.5 eV, due to loss of non-bridging oxygen (NBO) atoms, i.e. the loss of Si-O-Ca moieties upon silicate polymerisation. Again, the changes in the spectra of the calcium-rich phases (C/S≥0.83) were more pronounced, with almost complete loss of intensity at 530.5 eV, and increased intensity at higher binding energies, due to the presence of Si-O-Si, Si-O-H and carbonate. The presence of these species agrees with Raman analyses, where extensive carbonation of the most calcium-rich C-S-H phases had occurred during storage for six months, with the formation of highly polymerised silicates (Q^4), which often comprised silanol (Si-OH) species [16].

In addition to changes associated with silicate polymerisation, ageing of the samples also led to changes in their C 1s spectra (Fig. 1c), with the appearance of a peak at ~290 eV, indicative of a carbonate species.[2] Carbonation was extremely slight for the calcium-poor phases, there being a carbonate peak just about visible in the C 1s spectra. The phases with C/S=0.83 and 1.00 carbonated to a slightly greater extent, whilst the two most calcium-rich phases (C/S=1.33 and 1.50) carbonated to a considerable degree. Extensive carbonation of these two samples was unsurprising, given that the fresh samples were found to contain portlandite [10,15]. However, the amount of carbonate formed could not be explained simply by carbonation of the portlandite, and decalcification of the C-S-H also occurred. This is in agreement with the observations by Raman spectroscopy, where C-S-H decalcification was clearly observed [16]. The calcium-rich phases with C/S ratios of 1.33 and 1.50 have been found, on the basis of their portlandite contents, determined by thermal analysis [28] and quantitative XRD [29], to actually have C/S ratios of 1.24 and 1.27. That these samples were found to readily decalcify is in agreement with the findings of Chen et al. [30], who showed that a C/S ratio of 1.2 marked the initial point when calcium ions could be removed from the interlayer of C-S-H during decalcification.

As well as binding energy shifts, there are other subtle spectral changes which illuminate the process of ageing. Photoelectrons emitted from just below a sample surface undergo inelastic scattering. These photoelectrons contribute to the background signal, so that subsurface elements present a more stepped baseline. The Ca 2p spectra of the samples with C/S=1.50 and 1.33 show such an increase in the stepped background after ageing, whilst the Si 2p and O 1s spectra show no such steps. This seems to suggest that the silica/silanol groups reside on the outermost surface, whilst the calcium, as carbonate, is slightly subsurface. It should be remembered however, that the analysis depth is 5–10 nm, so despite the carbonate species being designated as subsurface, for detection it must still be present in the topmost 5–10 nm.

Analysis of the fresh phases had revealed a good correlation between bulk C/S ratio and the surface C/S ratio as measured by XPS [10]. This was not the case for the aged samples. Fig. 2a shows how the surface C/S, i.e. the topmost 5–10 nm measured by XPS, varies with the bulk C/S for the fresh and aged phases. The discrepancy between the measured and the bulk C/S ratios of the aged samples in particular is further evidence of the formation of a silicon-rich outer surface layer, with the carbonate being slightly subsurface. We consider there to be two possible reasons behind this observation. On a compositional

[2] Note: the peak at 2.84.8 eV in every spectra is due to carbon contamination from the vacuum systems. This peak is omnipresent in photoelectron spectra and is known as 'adventitious carbon' due to its function as in internal energy standard. This peak is slightly broader in the spectra from the aged samples due to the build up of contamination during the ageing of the samples.

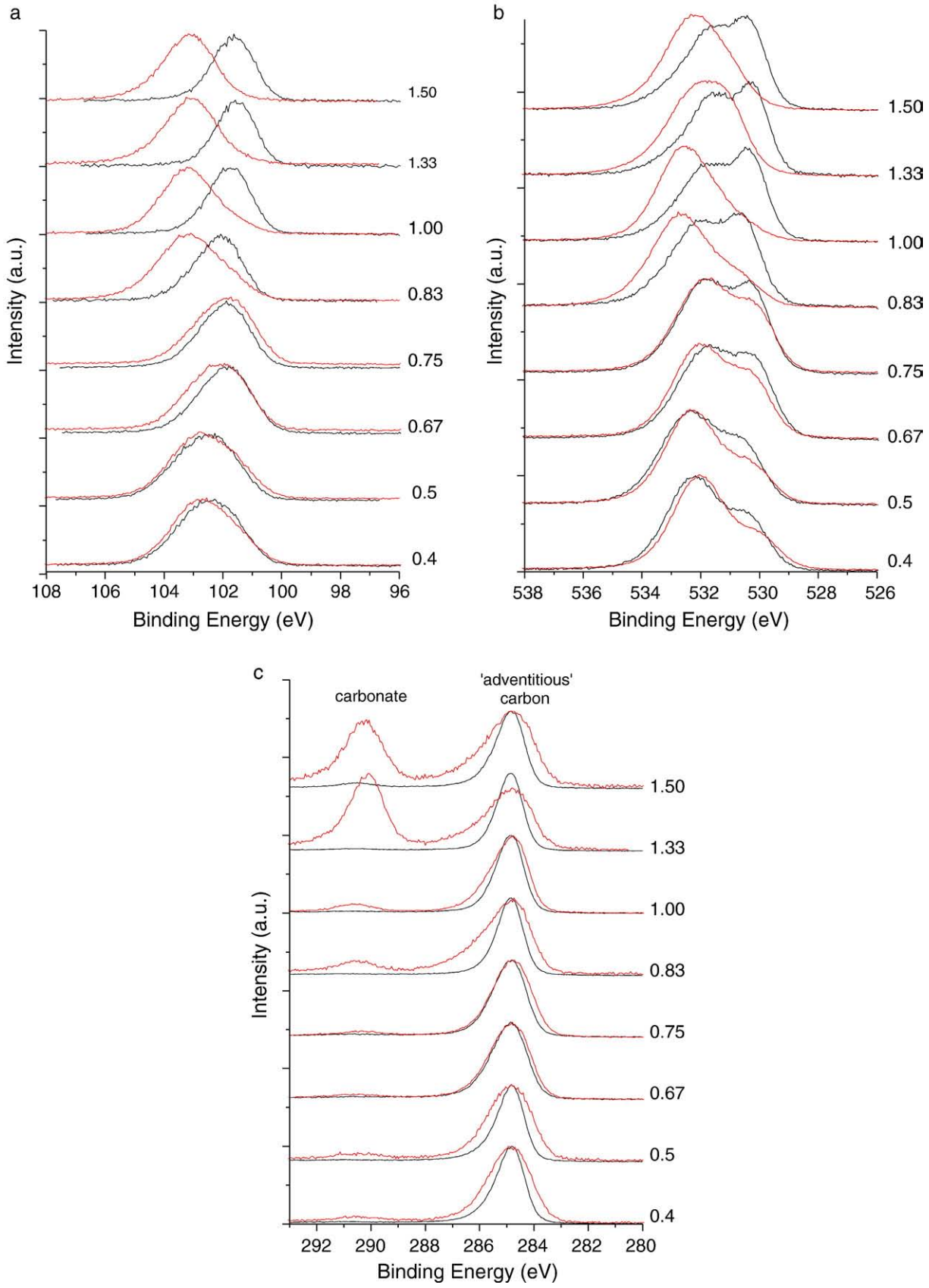

Fig. 1. Photoelectron spectra for the fresh (black) and aged (red) C-S-H samples with C/S 0.4 to 1.5. a) Si 2p b) O 1s. c) C 1s.

level, the carbonated sample may be considered as a series of carbonate crystals dispersed in an amorphous silica matrix. In which case, the smaller silica particles will be preferentially be found on the sample surface. The observation may also be explained structurally. Carbonation is a process which takes place in the presence of water. Whilst our samples have been dried, there is still structural water

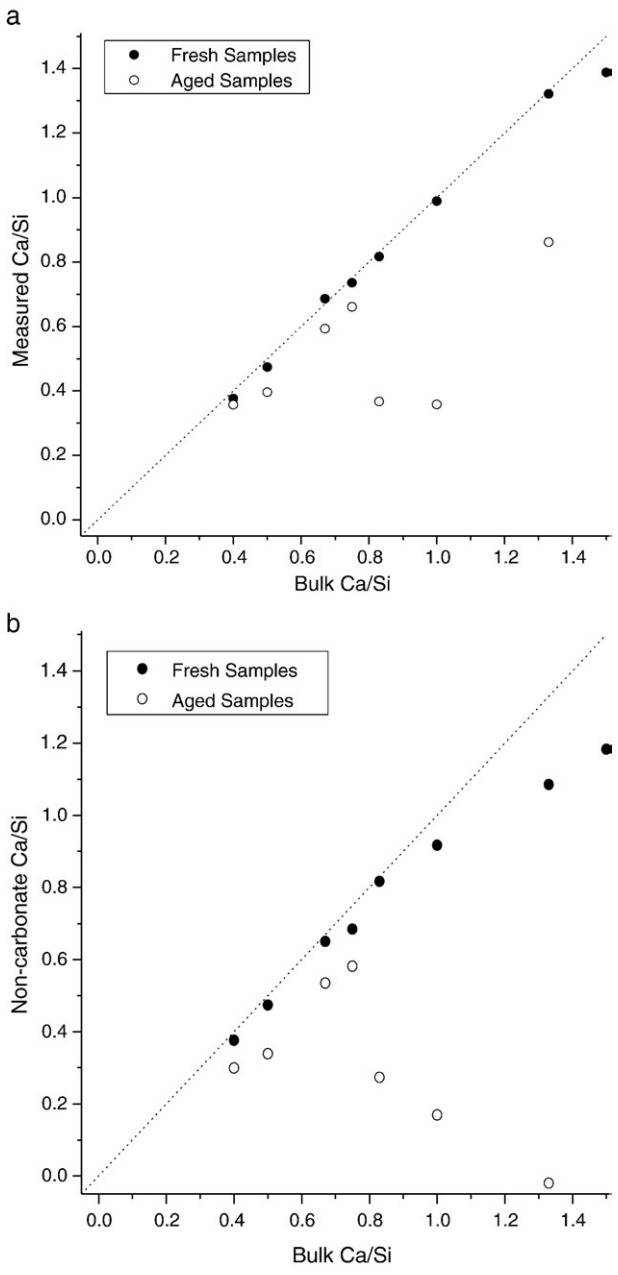

Fig. 2. Plots of surface Ca/Si, as measured by XPS, versus bulk Ca/Si for the fresh and aged C-S-H samples. a) simple relationship between surface and bulk Ca/Si ratio b) Ca/Si ratio within the C-S-H phases versus bulk Ca/Si ratio, i.e. after correcting surface Ca/Si for the presence of calcium carbonate.

within the C-S-H interlayer, where carbonation could occur. Carbonation of the calcium-rich phases has been shown previously to result in formation of amorphous calcium carbonate, vaterite and hydrated silica [16]. The carbonate phases have higher surface energies than silica [31], especially when the silica is hydrated. Therefore, minimisation of surface energy would result in surface segregation with the silica above the carbonate.

Fig. 2b shows the measured C/S ratio, after subtraction of any calcium associated with carbonate. The phases with C/S≤0.75 had decalcified slightly, leading to the slight shift in Si 2p binding energy seen in Fig. 1. The samples with C/S=0.83 and 1.00 had decalcified considerably, resulting in partial, but not complete, silicate anion polymerisation. This resulted in a shift in the Si 2p binding energy to give maxima at 103.2 eV, but there was still some residual intensity at ~102 eV. For the two most calcium-rich phases, decalcification was

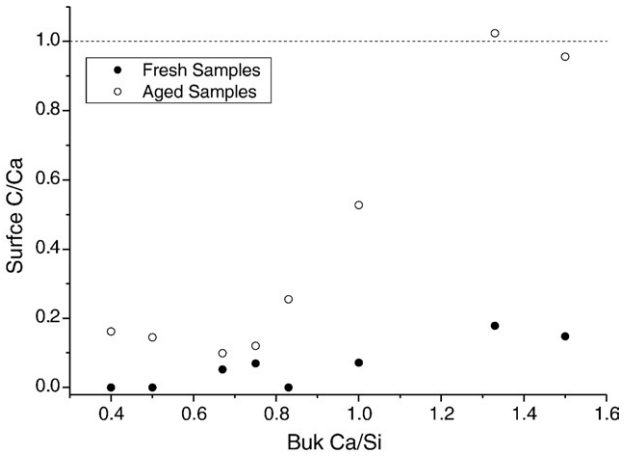

Fig. 3. Variation in the calcium carbonate ratio with bulk Ca/Si ratio, for the fresh and aged C-S-H samples.

complete, and the silicon was present as silica and/or silanol species. The importance of this finding, that the surface C/S ratio is not the same as the C/S ratio of the aged C-S-H phases, is important when considering the structure of the aged, decalcified C-S-H phases.

Fig. 3 shows the variation in C/Ca ratio for the fresh and aged samples. This figure confirms that the aged calcium-rich phases were completely decalcified after storage for six months. Approximately 30

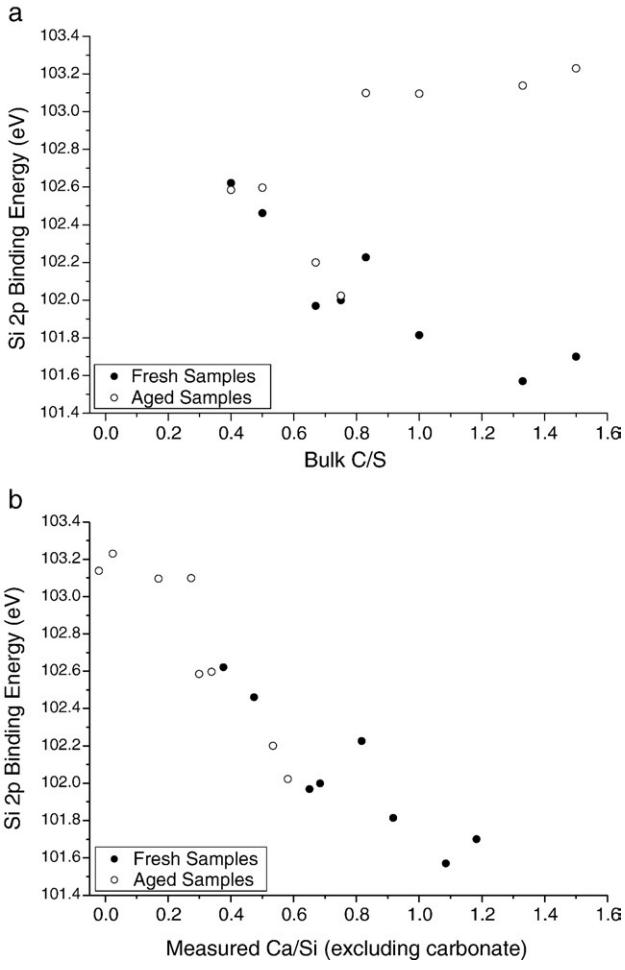

Fig. 4. Variation in Si 2p binding energy with Ca/Si for the various fresh and aged C-S-H samples. a) bulk Ca/Si a) surface Ca/Si (i.e. excluding carbonate).

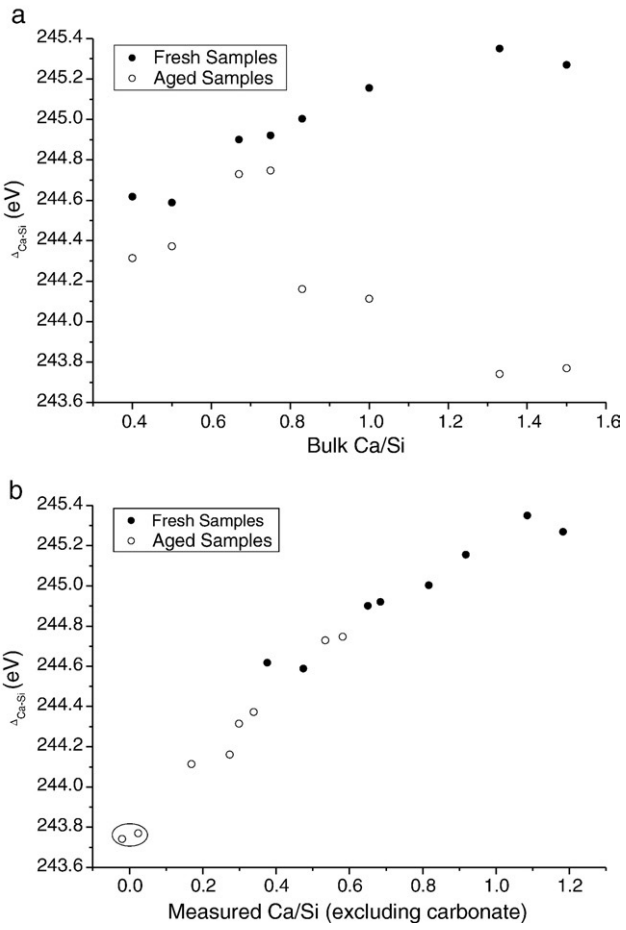

Fig. 5. Variation in $\Delta_{Ca\text{-}Si}$ with Ca/Si for the various fresh and aged C-S-H samples. a) bulk Ca/Si b) surface Ca/Si (i.e. excluding carbonate).

and 50% of the calcium was present as calcium carbonate in the samples with C/S=0.83 and 1.00 respectively. This figure fell to between 10 and 20% for the more calcium-depleted phases, with a minimum for C/S=0.67. This agrees with the Raman analysis of these samples, where carbonation was minimal for the samples with C/S=0.67 and 0.75 [16].

Fig. 4a and b shows the variation in Si 2p binding energies with C/S before and after ageing. Fig. 4a illustrates how it was the phases with C/S≥0.83 which underwent considerable change upon storage, with a shift in binding energy indicative of the formation of Q^4 units. The calcium-depleted phases did not appear to undergo much structural change. However, the breadth of the Si 2p peaks for the calcium-depleted phases were such that there was intensity at ~103 eV, indicating that Q^4 species could have been present. This was not the case for the samples with C/S=0.67 and 0.75, which also underwent minimal changes upon storage but still, on the basis of their binding energies, did not contain any Q^4 silicate species. This agrees with the observations from Raman spectroscopy, where Q^4 species were observed for all of the phases, with the exception of those with C/S=0.67 and 0.75, after storage for six months.

Fig. 4b shows how the Si 2p binding energies show a strong negative correlation with C/S, as has been demonstrated previously [6,10]. Carbonation, and the subsequent decalcification, leads to silicate polymerisation, to yield eventually Q^4 silicates and/or silanol species.

A more accurate measure of the degree of silicate polymerisation is the energy separation between the Si 2p and the Ca $2p_{3/2}$ peaks ($\Delta_{Ca\text{-}Si}$). This has previously been used to follow silicate polymerisation upon hydration of C_3S [3] and C_2S [4], there being a decrease in energy separation upon hydration, i.e. silicate polymerisation. Fig. 5a and b shows the variation in $\Delta_{Ca\text{-}Si}$ with C/S for the fresh and aged samples. Fig. 5a illustrates clearly how the different phases behaved very differently, with the calcium-rich samples undergoing the greatest structural change, the dimeric silicate groups [15] polymerising completely to yield Q^4 silicate units. The samples with C/S=0.83 and 1.00 polymerised considerably, but not completely. Noticeable changes were also seen in the structures of the samples with C/S=0.4 and 0.5, with the formation of more highly polymerised silicate units. The samples with C/S=0.67 and 0.75 did polymerise slightly, but less than any of the other samples, in agreement with the results obtained by Raman spectroscopy [16].

Fig. 5b clearly illustrates how the extent of silicate polymerisation is related to the C/S of the aged C-S-H. Note that the two marked data points correspond to the samples with bulk C/S ratios of 1.33 and 1.50 which had decalcified completely to yield a mixture of silica and calcium carbonate, giving a somewhat artificial value for $\Delta_{Ca\text{-}Si}$.

4. Conclusions

X-ray photoelectron spectroscopy has effectively been used to follow the effects of surface carbonation of a series of synthetic calcium silicate hydrates. Formation of calcium carbonate was observed on the topmost 5–10 nm of most samples, but was particularly pronounced on calcium-rich samples (with C/S ratios of 1.33 and 1.50). In addition to the formation of calcium carbonate, decalcification of the C-S-H was observed. Again, this was most pronounced for the calcium-rich phases, where decalcification was complete and a silica gel was formed. However, decalcification was also observed for the most calcium-poor phases, where there was increased silicate polymerisation, but some calcium remained in the C-S-H structure. C-S-H decalcification was least for the fresh samples with C/S=0.67 and 0.75.

There appeared to be a 'jump' in carbonation behaviour between C/S=0.75 and 0.83. This is the point, compositionally, where there is a change in C-S-H structure. For C/S ratios of 0.67 and 0.75 the C-S-H comprises of long dreierketten chains, with no interlayer calcium. With increasing calcium content there is increasing structural disorder, with the appearance of dimeric silicates and calcium in the interlayer, the presence of which allows ready carbonation.

Raman analysis of the fresh samples has revealed that the calcium-rich phases, and in particular the phases with C/S=1.33 and 1.50, contained a large number of dimeric silicate anions [15]. It was these samples which were the most susceptible to decalcification, indicating that the silicate dimer is not particularly stable. Whilst silicate polymerisation upon cement hydration yields dimers, then ever lengthening chains, with Q^3 sheets having been observed in slightly carbonated pastes, this did not occur with our samples. Rather, there was the direct decalcification of dimeric and chain silicates (depending upon the initial C/S ratio) to yield a silica gel. We assume this to be due to the samples being dried and then stored under ambient conditions, i.e. with no pore water present.

These findings support the mechanism proposed by Chen et al. when considering decalcification shrinkage [32]. Decalcification leads to an excess negative charge, which may be balanced by protonation, and the formation of silanol (Si-OH) groups, as suggested by the O 1s spectra. Neighbouring silanol groups may then condense with the ejection of water, leading to a more highly polymerised silicate, as seen in the Si 2p spectra.

Earlier analyses had shown the fresh samples to possess a tobermorite-like structure, with the calcium-rich phases with C/S ratios of 1.33 and 1.50 also containing portlandite. The presence of structural features readily susceptible to decalcification indicate considerable defects within the tobermorite-like structure. In this respect, the mechanochemically prepared synthetic C-S-H phases used in this study may be considered to possess defect-tobermorite

structures, similar to the model suggested by Stade and Wieker [20] and Cong and Kirkpatrick [21]. It is entirely reasonable to assume that mechanochemical synthesis of C-S-H phases yields tobermorite-like structures given Saito's use of this method to produce tobermorite [27].

Acknowledgements

LB and IG would like to acknowledge the support of EPSRC (grant reference EP/E025722/1) for supporting this work through the Daresbury NCESS Facility. They would also like to thank Dr. Danny Law for his support at NCESS. Finally, thanks go to Marc Bornefeld, FZK-ISS for his assistance with the sample synthesis.

References

[1] M.F. Hochella Jr., in: F.C. Hawthorne (Ed.), Spectroscopic Methods in Mineralogy and Geology, Reviews in Mineralogy, vol. 18, Mineralogical Society of America, Washington DC, 1988, pp. 573–637.
[2] Leon Black, Andreas Stumm, Krassimir Garbev, Peter Stemmermann, Keith R. Hallam, Geoffrey C. Allen, X-ray photoelectron spectroscopy of the cement clinker phases tricalcium silicate and β-dicalcium silicate, Cem. Concr. Res. 33 (2003) 1561–1565.
[3] M. Regourd, J.H. Thomassin, P. Baillif, J.C. Touray, Study of the early hydration of Ca_3SiO_5 by X-ray photoelectron spectrometry, Cem. Concr. Res. 10 (1980) 223–230.
[4] J.H. Thomassin, M. Regourd, P. Baillif, J.C. Touray, Étude de l'hydratation initiale du silicate bicalcique β par spectrométrie de photoélectrons, C. R. Acad. Sci. Paris 290 (1980, Jan.) 1–3.
[5] D. Ménétrier, I. Jawed, T.S. Sun, J. Skalny, ESCA and SEM studies on early C3S hydration, Cem. Concr. Res. 9 (1979) 473–482.
[6] A. Stumm, K. Garbev, G. Beuchle, L. Black, P. Stemmermann, R. Nüesch, Formation of C-S-H (I) and its hydrothermal analogue gyrolite in the system CaO-ZnO-SiO_2-H_2O, Cem. Concr. Res. 35 (2005) 1665–1675.
[7] L. Black, A. Stumm, K. Garbev, P. Stemmermann, K.R. Hallam, G.C. Allen, X-ray photoelectron spectroscopy of aluminium-substituted tobermorite, Cem. Concr. Res. 35 (1) (2005) 51–55.
[8] L. Black, K. Garbev, P. Stemmermann, K.R. Hallam, G.C. Allen, Characterisation of crystalline C-S-H phases by X-ray Photoelectron Spectroscopy (XPS), Cem. Concr. Res. 33 (6) (2003) 899–911.
[9] L. Black, K. Garbev, P. Stemmermann, K.R. Hallam, G.C. Allen, Erratum to "characterisation of crystalline C-S-H phases by X-ray Photoelectron Spectroscopy (XPS), Cem. Concr. Res., vol 33(6), (2003), pp.899–911", Cem. Concr. Res. 33 (11) (2003) 1913.
[10] L. Black, K. Garbev, G. Beuchle, P. Stemmermann, D. Schild, X-ray photoelectron spectroscopic investigation of nanocrystalline calcium silicate hydrates synthesised by reactive milling, Cem. Concr. Res. 36 (2006) 1023–1031.
[11] K. Okada, Y. Kameshima, A. Yasumori, Chemical shifts of silicon X-ray photoelectron spectra by polymerization structures of silicates, J. Am. Ceram. Soc. 81 (7) (1998) 1970–1972.
[12] H. Seyama, M. Soma, Bonding-state characterization of the constituent elements of silicate minerals by X-ray photoelectron spectroscopy, J. Chem. Soc. Faraday Trans. 81 (1985) 485–495.
[13] C.D. Wagner, D.E. Passoja, H.F. Hillery, T.G. Kinsky, H.A. Six, W.T. Jansen, J.A. Taylor, Auger and photoelectron line energy relationships in aluminum- oxygen and silicon- oxygen compounds, J. Vac. Sci. Technol. 21 (4) (1982) 933–944.
[14] L. Black, K. Garbev, P. Stemmermann, K.R. Hallam, G.C. Allen, X-ray Photoelectron Study of oxygen bonding in crystalline C-S-H phases, Phys. Chem. Miner. 31 (2004) 337–346.
[15] K. Garbev, P. Stemmermann, L. Black, C. Breen, J. Yarwood, B. Gasharova, Structural features of C-S-H(I) and its carbonation in air—a Raman spectroscopic study. Part I: fresh phases, J. Am. Ceram. Soc. 90 (3) (2007) 900–907.
[16] L. Black, C. Breen, J. Yarwood, K. Garbev, P. Stemmermann, B. Gasharova, Structural features of C-S-H(I) and its carbonation in air—a Raman spectroscopic study. Part II: carbonated phases, J. Am. Ceram. Soc. 90 (3) (2007) 908–917.
[17] H.F.W. Taylor, Proposed structure for calcium silicate hydrate gel, J. Am. Ceram. Soc. 69 (1986) 464–467.
[18] H.F.W. Taylor, Tobermorite, jennite, and cement gel, Z. Kristallogr. 202 (1992) 41–50.
[19] K. Fujii, W. Kondo, Estimation of thermochemical data for calcium silicate hydrate (C-S-H), J. Am. Ceram. Soc. 66 (12) (1983) 220–221.
[20] H. Stade, W. Wieker, Zum Aufbau schlecht geordneter Calciumhydrogensilicate. I. Bildung und Eigenschaften einer schlecht geordneten Calciumhydrogendisilicatphase, Z. Anorg. Allg. Chem. 466 (1980) 55–70.
[21] X.D. Cong, R.J. Kirkpatrick, 29MAS NMR study of the structure of calcium silicate hydrate, Adv. Cem. Based Mater. 3 (3/4) (1996) 144–156.
[22] I.G. Richardson, Tobermorite/jennite- and tobermorite/calcium hydroxide-based models for the structure of C-S-H: applicability to hardened pastes of tricalcium silicate, β-dicalcium silicate, Portland cement, and blends of Portland cement with blast-furnace slag, metakaolin, or silica fume, Cem. Concr. Res. 34 (9) (2004) 1733–1777.
[23] K. Kobayashi, K. Suzuki, Y. Uno, Carbonation of concrete structures and decomposition of C-S-H, Cem. Concr. Res. 24 (1) (1994) 55–61.
[24] G.W. Groves, D.K. Rodway, I.G. Richardson, The carbonation of hardened cement pastes, Adv. Cem. Res., 3 (11) (1990) 117–127.
[25] G.W. Groves, A.R. Brough, I.G. Richardson, C.M. Dobson, Progressive changes to the structure of hardened C3S cement pastes due to carbonation, J. Am. Ceram. Soc. 74 (11) (1991) 2891–2896.
[26] N.R. Short, A.R. Brough, A.M.G. Seneviratne, P. Purnell, C.L. Page, Preliminary investigations of the phase composition and fine pore structure of super-critically carbonated cement pastes, J. Mater. Sci. 39 (2004) 5683–5687.
[27] F. Saito, G. Mi, M. Hanada, Mechanochemical synthesis of hydrated calcium silicates by room temperature grinding, Solid State Ion. 101–103 (1997) 37–43.
[28] K. Garbev, G. Beuchle, M. Bornefeld, P. Stemmermann, Cell dimensions and composition of nanocrystalline calcium silicate hydrate solid solutions. Part 2: X-ray and thermogravimetry study, J. Am. Ceram. Soc. submitted for publication.
[29] K. Garbev, G. Beuchle, M. Bornefeld, L. Black, P. Stemmermann, Cell dimensions and composition of nanocrystalline calcium silicate hydrate solid solutions. Part 1: synchrotron based X-ray diffraction, J. Am. Ceram. Soc. submitted for publication
[30] J.J. Chen, J.J. Thomas, H.F.W. Taylor, H.M. Jennings, Solubility and structure of calcium silicate hydrate, Cem. Concr. Res. 34 (2004) 1499–1519.
[31] J.M. Douillard, T. Zoungrana, S. Partyka, Surface Gibbs free energy of minerals: some values, J. Petrol. Sci. Eng. 14 (1–2) (1995) 51–57.
[32] J.J. Chen, J.J. Thomas, H.M. Jennings, Decalcification shrinkage of cement paste, Cem. Concr. Res. 36 (2006) 801–809.